

¹Effect of Energy Dependent Cross-section on Flow Velocity Measurements with Charge Exchange Spectroscopy in Magnetized Plasma

J. Chen^{a,*}, K. Ida^{b,c}, M. Yoshinuma^{b,c}, I. Murakami^{b,c}, T. Kobayashi^{b,c}, M.Y. Ye^a, B. Lyu^d

^a *School of Physical Sciences, University of Science and Technology of China, Hefei 230026, China*

^b *National Institute for Fusion Science, National Institutes of Natural Sciences, Toki, Gifu 509-5292, Japan*

^c *SOKENDAI (The Graduate University for Advanced Studies), Toki, Gifu 509-5292, Japan*

^d *Institute of Plasma Physics, Chinese Academy of Sciences, Hefei 230031, China*

ABSTRACT

Charge exchange spectroscopy (CXS) is widely used to measure plasma flow velocity. Accurate measurement is heavily affected by energy dependent cross section between neutral atoms and impurity ions. One symmetric layout of poloidal CXS is applied on Large Helical Device. Correction velocity due to the cross section is exacted from total velocity when actual plasma flow velocity is acquired with the benefit of this layout. A linear relationship between correction velocity and ion temperature is observed. Abundant discharges with wide plasma conditions are investigated and the ratio of correction velocity to ion temperature with the same beam energy shows the normal distribution. The impact of beam energy on the ratio of correction velocity to ion temperature of the carbon system and the hydrogen system is discovered based upon the statistics. Effective emission coefficient (Q) from Atomic Data and Analysis Structure (ADAS) is utilized to study the dependence of correction velocity on Q . The relationship in which the ratio of correction velocity to ion temperature increases linearly with the increasing normalized effective emission coefficient ($(1/Q)dQ/dv$) is observed. Experimental $(1/Q)dQ/dv$ is obtained according to this observation, and comparison with different fractions of $n=2$ excited state is also discussed. The influence of different receivers (carbon and hydrogen) is also presented. The experimental $(1/Q)dQ/dv$ from the carbon system decreases with beam energy decreasing when beam energy is less than 30 keV/amu. This tendency of $(1/Q)dQ/dv$ at low beam energy indicates the existence of the contribution of $n=2$ excited state donors to the cross section.

Keywords: charge exchange spectroscopy, flow velocity, cross section, excited state

*Trainee of National Institute for Fusion Science internship training program

1. Introduction

Plasma rotation and its shear have been recognized as being critical to the improvement of plasma confinement [1, 2]. Accurate measurements of the flow velocity are required for better interpretation of plasma rotation. In present fusion devices, plasma flow velocity is mainly measured by CXS based on the Doppler shift of a special line [3-5]. The line, ideally, is in Maxwell-Boltzmann distribution due to the thermal motion of ions. However, the distribution is distorted by the charge exchange process between impurity ions and the incoming atoms from neutral beam injection (NBI) because of the energy dependent cross section, which results in an apparent line shift different from that resulting from plasma flow [6-9]. As a result, the measured rotation is the combination of the actual plasma flow velocity and the correction velocity V_{cor} associated with the cross section. Actually, V_{cor} relies on some parameters of plasma and NBI, such as beam energy, ion temperature, density, and plasma rotation. But among them, ion temperature and beam energy play the most important roles. It is found that V_{cor} increases with ion temperature and could reach a few tens km/s which is in the same order of the intrinsic rotation in high ion temperature plasma. As for beam energy, it usually affects V_{cor} by changing the operation point on the cross section. It is noticed that the cross section of $n=2$ excited state peaks and becomes increasingly important at low beam energy even though the fraction of $n=2$ excited state is only 0.05%~0.4% [10]. Consequently, the contribution of the cross section of $n=2$ excited state to flow velocity measurements should be also considered at low beam energy.

In previous work, the cross section calculated by Atomic Data and Analysis Structure (ADAS) is applied to correct flow velocity measurements [6, 7, 9, 11]. However, there remains disagreement with experiments in various plasma conditions. Some direct measurements of flow velocity without depending on the cross section calculations are also developed [9, 11]. More attention is paid to the accuracy of the correction with calculations. Given that the cross section is sensitive to the excited state population of the neutral beam [12, 13], it may be insufficient to use the calculated correction relying on the ADAS, especially when the beam energy is lower than 40 keV/amu, where the contribution of $n=2$ excited state to the cross section becomes significant. Therefore, in order to evaluate the true flow velocity, it is necessary to understand the characteristics of V_{cor} from experiments, which is also one test of the cross section with different atomic models.

A set of poloidal CXS system that has the ability to determine V_{cor} has been installed on Large Helical Device (LHD), laying a foundation for investigating the effect of the cross section on flow velocity measurements. In this paper, the geometry of the poloidal CXS and how one can determine V_{cor} from this symmetric layout are described. The relationship between V_{cor} and beam energy which reflects the structure of the cross section is also obtained.

2. Experimental setup

Poloidal CXS on LHD consists of two sets of optical systems. These sets are located above and below neutral beam BL4 in order to view the downward and the upward at the poloidal cross section as shown in Fig. 1 (a) [4]. The observation radii of the channel viewing downward are arranged to be between those of the channel viewing upward. Therefore, as shown in Fig. 1 (b) and (c), Doppler shift in the upward view and that in the downward view due to poloidal flow are in the opposite direction. However, the line shift due to the cross section is shown in another way. Fig. 1 shows how the cross section affects the measured impurity spectra. When the neutral beam is directed radially inward, the cross section of the ions moving toward the neutral atoms is different from that of the ions moving away from neutral atoms, causing a net line shift in the radial direction. The velocity corresponding to the net line shift is called correction velocity V_{cor} .

In the poloidal cross section, it can be seen from Fig. 1 (a) that there are some components of V_{cor} in the direction of line of sight for poloidal CXS so that V_{cor} can be measured by the diagnostic. It should be mentioned that flow velocity measurement is still influenced by V_{cor} even from the line of sight perpendicular to the neutral beam due to the gyro motion of the excited impurity ion in the finite lifetime [8, 9]. For the typical discharge on LHD, the toroidal magnetic field B_t at the magnetic axis is about 2.75 T, then the gyro frequency of excited carbon ion is $\omega = 1.1 \times 10^8$ Hz. The direction of V_{cor} will be redirected by $\omega\tau = 0.11$ ($\sim 6.3^\circ$) in the vertical direction for a lifetime τ of about 1 ns. Although the gyro motion will introduce a vertical component of V_{cor} ($V_{\text{perp}}^{\text{cor}}$) of about 10% in such a condition, the radial component of V_{cor} along the neutral beam is still 99.4% and can be considered approximately equal to V_{cor} . Therefore, the directions of $V_{\text{perp}}^{\text{cor}}$ show the same property of the poloidal flow and are opposite in the symmetric downward and upward views, but radial component of V_{cor} is the same for the views. Namely, line shifts due to the radial component of V_{cor} in the neighboring channels are the same. It should be noticed that the line shift in the radial direction is correction velocity due to the cross section effect because the radial flow velocity in the plasma is almost zero. As a result, on the one hand, the difference of the position of the central line in the neighboring channels represents the effect of Doppler shift due to poloidal flow plus line shift due to the vertical component of V_{cor} resulting from gyro motion of excited impurity ion with finite lifetime. On the other hand, the difference of the position of the absolute wavelength and the average position of the central line in the neighboring channels denotes the contribution of the cross section effect. For example, if the positions of the central line of neighboring channels are X_1 and X_2 , the sum of Doppler shift and the vertical component of V_{cor} can be expressed as $X_D + X_{\text{perp}}^{\text{cor}} = (X_1 - X_2)/2$ and the line shift due to the radial component of V_{cor} is $X_{\text{para}}^{\text{cor}} = (X_1 + X_2)/2 - X_0$, where X_0 is the position of the absolute wavelength without Doppler shift and the cross section effect. Though

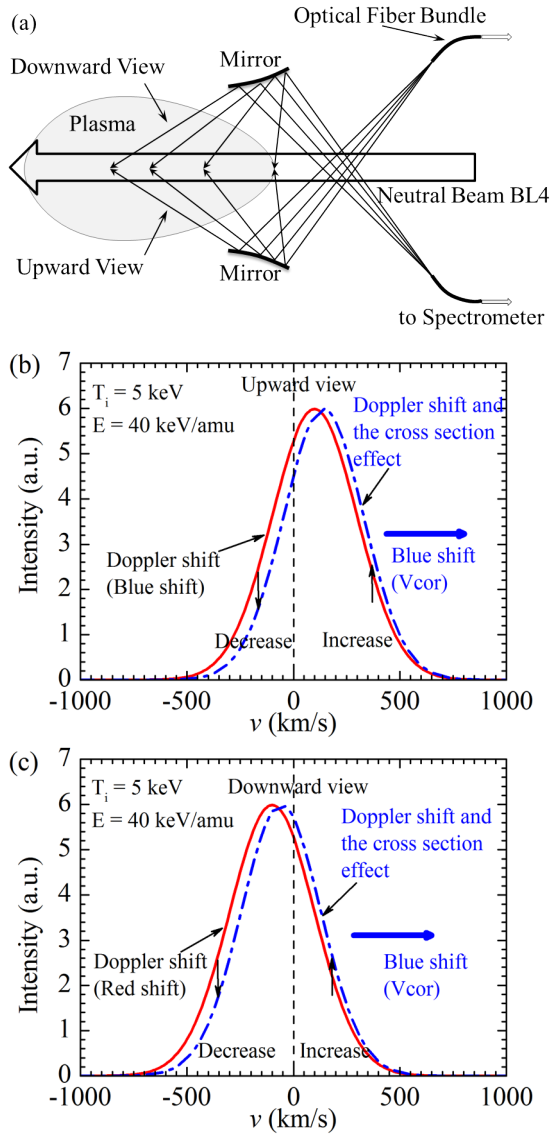


Fig. 1. Optical layout of poloidal CXS (a) and line shift due to Doppler shift and the cross section effect in upward view (b) and in downward view (c).

what is measured from poloidal CXS is the radial component of V_{cor} , this radial component can be regarded as V_{cor} due to the small difference between the values of them in such experimental conditions on LHD. As a result, the line shift due to the cross section effect X_{cor} can be considered as $X_{\text{para}}^{\text{cor}}$.

On LHD, the poloidal CXS has the ability to determine plasma parameters with the spectra of carbon and hydrogen. There are 24 and 16 channels for each viewing of the carbon system and the hydrogen system, respectively. Ion temperature and correction velocity due to the cross section used here are based on the spectra of charge-exchange line of carbon (CVI, $\lambda = 529.05$ nm), deuterium ($\text{D}\alpha$, $\lambda = 656.1$ nm) and hydrogen ($\text{H}\alpha$, $\lambda = 656.2$ nm). For hydrogen spectra, discharges with pure deuterium and hydrogen are analyzed because $\text{D}\alpha$ and $\text{H}\alpha$ overlap each other due to the close wavelength in the mixture of deuterium and hydrogen discharge. There are four sets of ion sources which can be hydrogen or

deuterium in BL4 and the beam energy can change from 30 keV to 60 keV. Therefore, beam energy per atom mass unit can be as low as 15 keV/amu, which provides an opportunity of revealing the effect of the cross section on flow velocity measurement at low beam energy. The data in this paper includes a wide plasma condition with ion temperature ranging from several hundreds of eV to 6 keV, electron temperature from several hundreds of eV to 10 keV, electron density from $0.4 \times 10^{-19} \text{ m}^{-3}$ to $5 \times 10^{-19} \text{ m}^{-3}$, toroidal magnetic field from 1.3 T to 2.85 T and beam energy from 19 keV/amu to 47 keV/amu.

3. Experimental results

Fig. 2 shows the time traces of ion temperature and V_{cor} in one channel. From 4.6 s to 4.8 s, ion temperature increases from 3 keV to 5 keV. It should be mentioned that the ion temperature is the observed ion temperature directly from poloidal CXS because the correction due to the cross section effect to ion temperature is negligible in the ion temperature range of the dataset. Meanwhile, the magnitude of V_{cor} shows the same tendency and increases from 60 km/s to 90 km/s in Fig. 2 (b), where the minus means that the direction is along the major radius and that the line shift is blue shift. Further, the magnitude of V_{cor} decreases with the decreasing ion temperature from 4.8 s to 5.1 s. In order to achieve a better understanding of the effect of ion temperature on V_{cor} , V_{cor} is plotted against ion temperature based on the data shown in Fig. 2. It is found that the magnitude of V_{cor} increases linearly with the

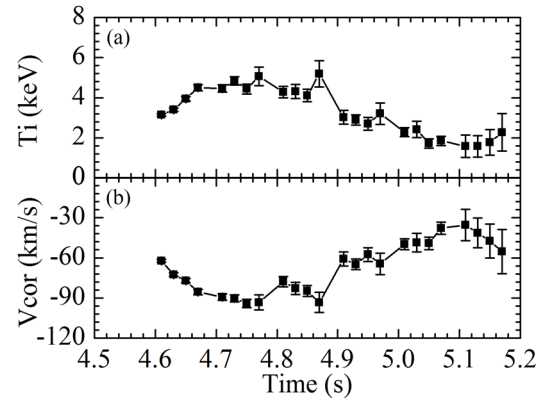


Fig. 2. Time traces of (a) ion temperature and (b) correction velocity for carbon in one channel of poloidal CXS

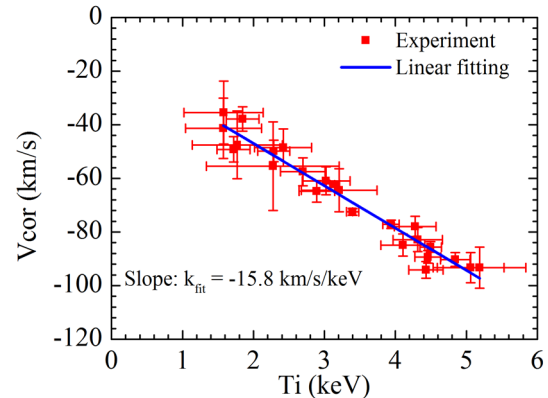


Fig. 3. The relationship between correction velocity and ion temperature for carbon

increasing ion temperature with the slope of -15.8 km/s/keV, as shown in Fig. 3. This dependence of V_{cor} on ion temperature can be clearly explained by the following process. Though the population of ions moving toward incoming neutral atoms is the same as that of ions moving away from neutral atoms, the average velocity of ions moving toward and away from neutral atoms in high ion temperature is larger than that in low temperature, which results in the increasing difference of the cross section between two parts with the increasing ion temperature. Then, effective emission coefficient which increases will continue increasing, but that which decreases will continue decreasing. At last, the line shift becomes larger in high ion temperature.

Although there are 48 channels in the carbon system of poloidal CXS, only 10 channels of each upward view and downward view in the core region are used because of the large errors of V_{cor} measurement in the edge resulting from the angle of the line of sight close to 90 degrees. As for the hydrogen system, 8 channels in the core region of 32 channels are utilized. It should be noted from linear fitting that V_{cor} is not equal to 0 when $T_i = 0$ and that the intercept of each channel changes from a negative value to a positive value when the channel moves from the core to the edge. This may result from the offset of the calibration. However, the offset does not have any influence on the slope of V_{cor} and T_i which represents the effect of T_i on V_{cor} because the offset is the same for each channel. It can be seen from the relationship between V_{cor} and T_i that correction velocity due to the cross section could be 15 km/s even with T_i of 1 keV. As a consequence, the effect of the cross section should be carefully considered to acquire accurate flow velocity when plasma rotation is measured by CXS, especially in high ion temperature discharge.

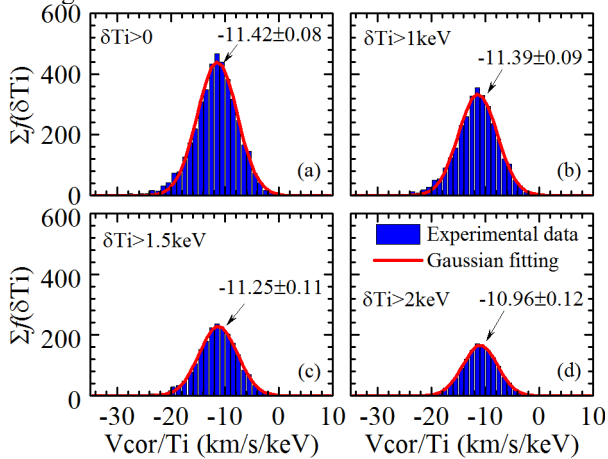


Fig. 4. Probability distribution function of the ratio of correction velocity to ion temperature of the carbon system when beam energy is 43.7 keV/amu with different ion temperature thresholds (a) 0 keV, (b) 1 keV, (c) 1.5 keV, and (d) 2 keV

The correction velocity is induced by the energy dependent cross section. How beam energy affects the correction velocity is one of the important issues for accurate flow velocity measurement. Considering that what contributes most to correction velocity is T_i and beam energy, it is necessary to distinguish the role of beam

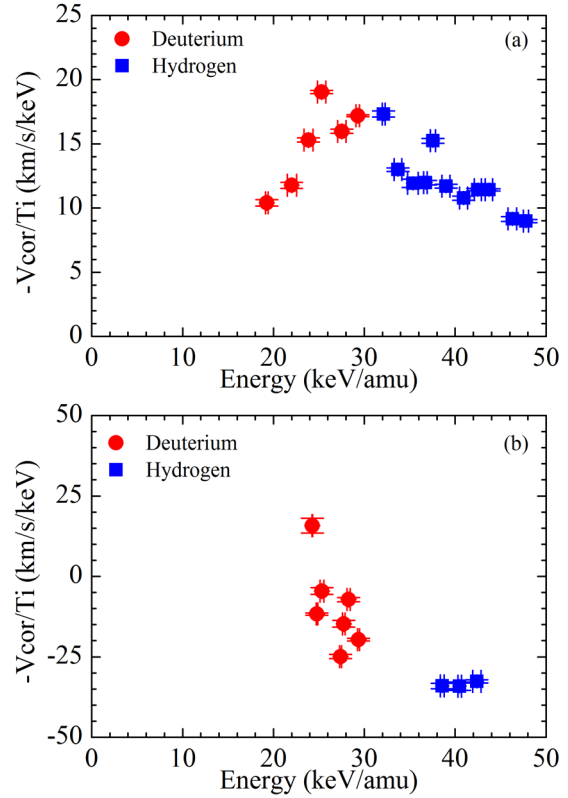


Fig. 5. The relationship between the ratio of correction velocity to ion temperature and beam energy (red circle and blue square are deuterium and hydrogen neutral beam source, respectively.) of (a) carbon and (b) hydrogen.

energy from that of T_i . The contribution of T_i to correction velocity is proportional to T_i and, ideally, the ratio of correction velocity to ion temperature V_{cor}/T_i should be a constant in one fixed beam energy with the same plasma parameters. Therefore, the dependence of correction velocity on beam energy can be determined by comparison with V_{cor}/T_i in different beam energy. Fig. 4 shows V_{cor}/T_i with beam energy of 43.7 keV/amu. Considering that the change of T_i varies with the channel (or major radius), one weight function f is applied to minimize the influence of linear fitting due to different ion temperature ranges. $f = \frac{1}{\delta T_i} - \frac{1}{\overline{\delta T_i}}$, where δT_i is the ion temperature range in each channel and $\overline{\delta T_i}$ is the average of all δT_i . V_{cor}/T_i is not a constant but walks randomly around one constant. There are about 200 shots in this statistic with V_{cor}/T_i changing from -28 km/s/keV to 2 km/s/keV. There are several reasons why V_{cor}/T_i changes in this wide range. One is that there are some measurement errors of T_i and correction velocity. Another is that other parameters except T_i and beam energy, such as ion density, ion effective charge, and the magnetic field, also have some influence on V_{cor} . As shown in Fig. 4, the effective count decreases with the increasing T_i threshold, while the difference between central V_{cor}/T_i calculated by Gaussian fitting with the minimum and maximum threshold of T_i is only 4%, which verifies the efficiency of the weighting function. In order to enhance the accuracy of the statistic, central V_{cor}/T_i of Gaussian fitting without T_i threshold is

thought of as V_{cor}/T_i with the same beam energy. On LHD, the density fractions of the full, half and one third energy for diagnostic beam are approximately 0.65, 0.15 and 0.2, respectively. The effective emission coefficient of half and one third energy is only about tens of percent of that of full energy. As a result, the emission population of the full energy is more than 90%. Therefore, full energy from neutral beam is chosen as beam energy because the contributions of half and one third energy to effective emission coefficient are very small compared with that of full energy. It should be noted that the fraction of beam energy component would vary slightly even with the same full energy when the operation parameter of the beam is modified. The variation of the fraction would result in a change of the effective emission coefficient because each component has different relative velocities and emission cross-section, which may be one of the possible candidates for the scatter of the measured V_{cor}/T_i .

The relationship between V_{cor}/T_i and beam energy is shown in Fig. 5. It is seen in Fig. 5 (a) that V_{cor}/T_i for the carbon system is positive, shows a peak against beam energy, and reaches the maximum at beam energy of 30 keV/amu. The minus in front of V_{cor}/T_i is applied to keep consistent with the definition of correction velocity in the calculation in next section. Because correction velocity is induced by the energy dependent cross section, the opposite tendency of V_{cor}/T_i implies the different changes of the cross section at two sides of the peak. By contrast, as shown in Fig. 5 (b), there is no peak for the hydrogen system. V_{cor}/T_i changes from the positive to the negative when beam energy increases from 24 keV/amu to 44 keV/amu and decreases monotonically with increasing beam energy. During the increase of beam energy, V_{cor}/T_i is 0 at one point, which means that there is no influence of the energy dependent cross section on the flow velocity measurement. The distinct difference of V_{cor}/T_i for the hydrogen system suggests another diverse cross section of hydrogen different from that of carbon.

4. Calculation of the dependence on effective emission coefficient

The spectrum measured by CXS is created by the excited state ions through charge exchange collisions between fully ionized ions and the neutral beam. However, the measurement suffers an additional apparent line shift due to the cross section effect. For poloidal flow velocity measurement, the gyro motion of the excited state ions also turns up because poloidal views are usually located at the poloidal plane. The actual velocity distribution function of the excited state ions can be described by the Boltzmann equation coupled with gyro motion as presented by Solomon *et al* [9] and Muñoz Burgos *et al* [14]. For the data in the paper, the toroidal magnetic field B_t is in the range of from 1.3 T to 2.85 T and the arc length which the excited state ions travel is about 0.05 ~ 0.11 with the lifetime of 1 ns. The effect of the gyro motion is negligible during the lifetime of the excited state ions. Therefore, the velocity distribution function of the excited ions can be considered as the product of the effective emission

coefficient and the velocity distribution function of fully ionized ions [15].

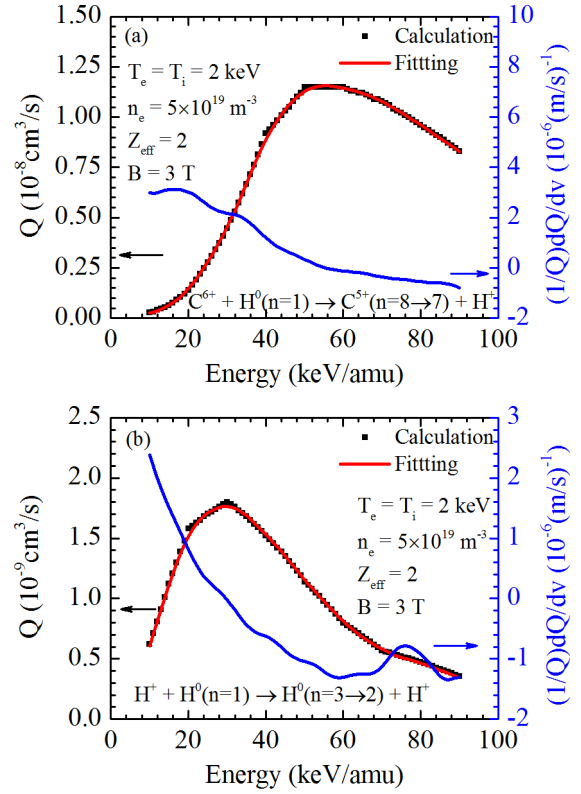


Fig. 6. Effective emission coefficient and its normalized gradient with the ground state donor calculated by ADAS database for (a) $C^{6+}+H^0(n=1)\rightarrow C^{5+}(n=8\rightarrow 7)+H^+$ and (b) $H^++H^0(n=1)\rightarrow H^0(n=3\rightarrow 2)+H^+$

The effective emission coefficient of fully ionized ions with velocity of \mathbf{v} can be expressed as $Q(|\mathbf{v}-\mathbf{V}_0|)$ where Q and \mathbf{V}_0 are effective emission coefficient and the velocity of neutral atoms, respectively. The distribution function of the excited state ions can be simply expressed as

$$f'(\mathbf{v}) = f(\mathbf{v}-\mathbf{v}_0)Q(|\mathbf{v}-\mathbf{V}_0|)/Q(|\mathbf{v}_0-\mathbf{V}_0|) \quad (1)$$

where $f(\mathbf{v})$ and \mathbf{v}_0 are the velocity distribution function of fully ionized ions and plasma flow velocity, respectively. It is noted that Doppler shift due to plasma rotation results from the movement of central velocity of $f(\mathbf{v}-\mathbf{v}_0)$ but that the cross section imparts on the line shift by redistributing the population of $f(\mathbf{v}-\mathbf{v}_0)$ through Q . The combined velocity of them can be regarded as the first order moment of $f'(\mathbf{v})$,

$$M1 = \int \mathbf{v} f'(\mathbf{v}) d\mathbf{v} / \int f'(\mathbf{v}) d\mathbf{v}. \quad (2)$$

If the velocity distribution function $f(\mathbf{v}-\mathbf{v}_0)$ is Maxwell-Boltzmann distribution and only one dimension is considered, bring eq. (1) into eq. (2), then

$$M1 = \mathbf{v}_0 \frac{\overline{Q(\mathbf{v}+\mathbf{v}_0+\mathbf{V}_0)}}{Q(\mathbf{v}_0+\mathbf{V}_0)} + \frac{kT_i}{m} \frac{1}{Q(\mathbf{v}_0+\mathbf{V}_0)} \frac{dQ(\mathbf{v}+\mathbf{v}_0+\mathbf{V}_0)}{d\mathbf{v}} \quad (3)$$

where the overline is the average of $\exp(-m\mathbf{v}^2/(2kT_i))$ and k , T_i and m are Boltzmann constant, ion temperature, and mass of fully ionized ions, respectively. Usually, thermal velocity is much smaller than the velocity of neutral atoms when ion temperature is not very high and Q can be represented as the second order Taylor expansion [15],

$$Q(v+V_0)=Q(V_0)+\left.\frac{dQ}{dv}\right|_{v=V_0}v+\left.\frac{d^2Q}{dv^2}\right|_{v=V_0}v^2. \quad (4)$$

As a result, the correction velocity $\delta v \approx M1 - v_0$ due to the cross section can be approximately expressed as

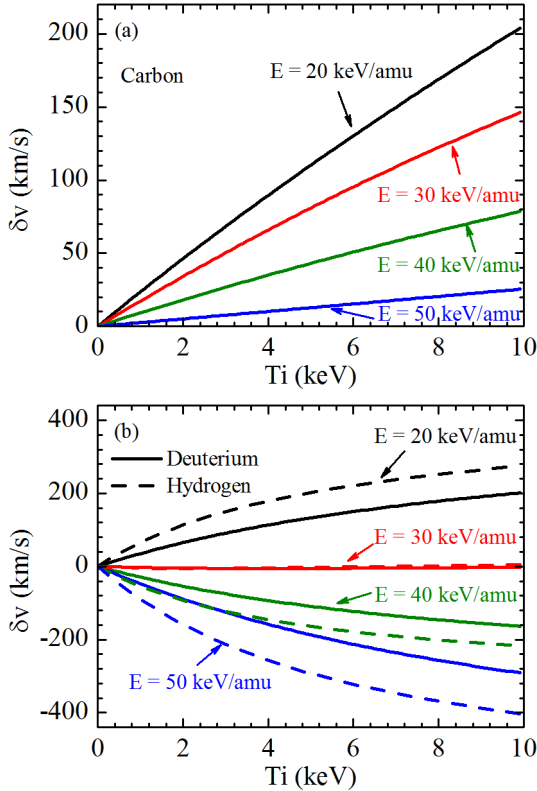
$$\delta v = \frac{kT_i}{mQ} \left[\frac{dQ}{dv} + \frac{3}{2}v_0 \frac{d^2Q}{dv^2} - \frac{v_0}{Q} \left(\frac{dQ}{dv} \right)^2 \left(\frac{mv_0^2}{kT_i} + 1 \right) \right] \quad (5)$$

where terms of higher order are omitted. The terms on the right side of eq. (5) denote the influence of the gradient of Q , the curvature of Q and the square of the gradient of Q , respectively. The contributions of the second and the third terms to correction velocity are about 10% of that of the first term and are almost compensated by each other at low energy. The contribution of the second term becomes significant at the peak of Q where the gradient of Q is very small and the curvature is large but the absolute value of the contribution is not very high because of the relatively small dependence of Q on beam energy at the peak region. The third term may come into play when $(1/Q)dQ/dv$ is large enough to enhance the influence at high beam energy. Therefore, the first term plays the major role in all beam energy and δv is described as

$$\delta v \approx (kT_i/m)(1/Q)dQ/dv. \quad (6)$$

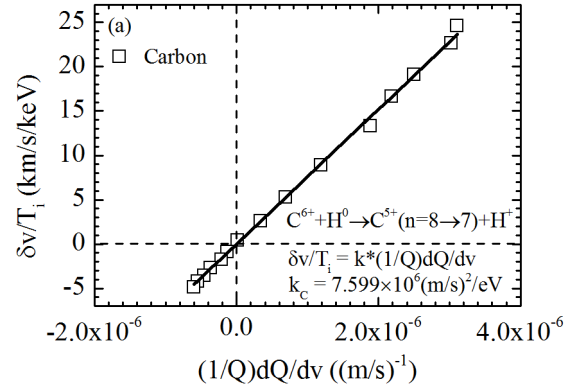
Derived from eq. (6), correction velocity increases linearly with the increasing ion temperature when the operation point $(1/Q)dQ/dv$ is fixed. In addition, it is interesting that what influences correction velocity is not effective emission coefficient itself but the normalized gradient of effective emission coefficient.

To evaluate δv quantitatively, effective emission coefficient Q calculated by ADAS [16] is applied to eq. (2). Fig. 6 shows effective emission coefficient between



receivers (carbon and hydrogen) and the ground state hydrogen and the normalized gradient. For the ground state, the preferred JET data “old” with medium/high quality in the library of qcx#h0 which has been produced from JET compilations is used to calculate Q . It is clear that Q can be divided into two regions, one with a positive gradient and another with a negative gradient. As shown in Fig. 6 (a), Q between carbon and hydrogen reaches the peak when beam energy is about 55 keV/amu and the normalized gradient $(1/Q)dQ/dv$ changes sign after passing the peak. And Q between hydrogen and hydrogen shown in Fig. 6 (b) peaks at lower beam energy compared with that between carbon and hydrogen. The change of the sign of $(1/Q)dQ/dv$ leads to the opposite line shift due to the cross section in the two regions based on eq. (6). On LHD, beam energy of BL4 is less than 60 keV/amu so that the operation point of the carbon system is in the positive region. However, the operation point of the hydrogen system can be in both regions in this condition.

As shown in Fig. 7, all of the absolute value of δv increase with the increasing ion temperature with different beam energies and the relationship between δv and ion temperature can be considered as linearity with ion temperature less than 10 keV, which is consistent with the experimental data shown in Fig. 3. In addition, δv from carbon spectra shown in Fig. 7 (a) is positive for all the beam energy. δv from deuterium spectra and hydrogen spectra change from the positive to the negative when beam energy increases from 30 keV/amu to 50 keV/amu, which is due to the reason that $(1/Q)dQ/dv$ changes sign in the range of beam energy. It should be mentioned that Q



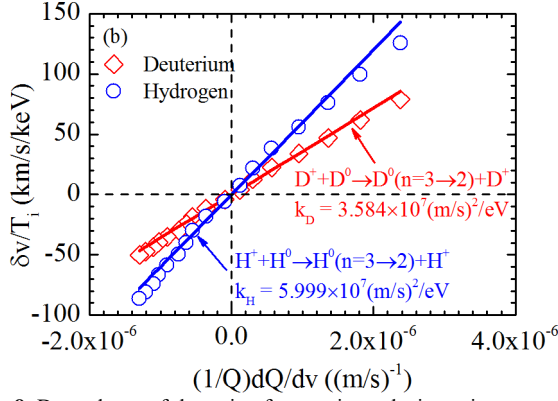


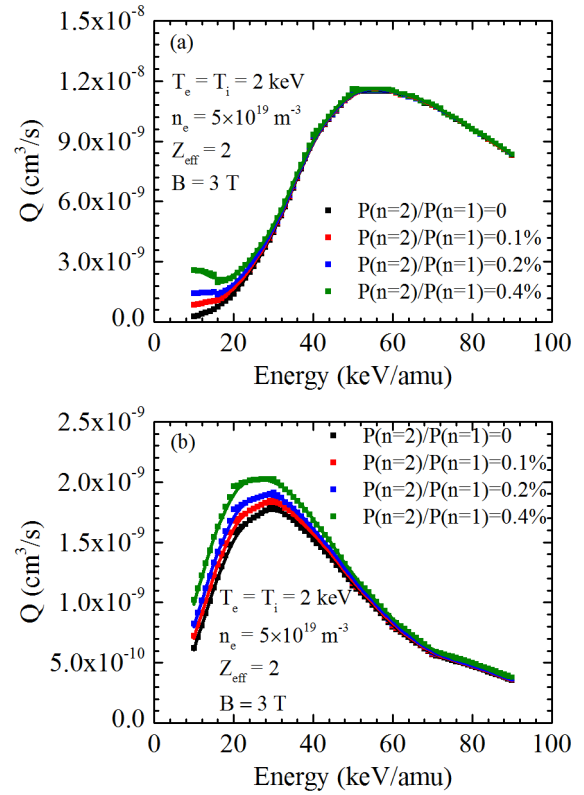
Fig. 8. Dependence of the ratio of correction velocity to ion temperature $\delta v/T_i$ on the normalized effective emission coefficient $(1/Q)dQ/dv$ (a) carbon and (b) deuterium and hydrogen

between deuterium and deuterium and that between hydrogen and hydrogen are the same. As shown in Fig. 7 (b), δv from deuterium spectra is larger than that from hydrogen spectra at the same beam energy, but not twice as large as that of hydrogen at high ion temperature, which is different from the conclusion from eq. (6). Returning to eq. (3), the average of Q and $(1/Q)dQ/dv$ is not determined by the local value at high ion temperature anymore and the influence of ion temperature on the average should be taken into account. Therefore, the variation occurs at high ion temperature. However, eq. (6) is still reasonable at low ion temperature. It also can be seen that the ratio of δv to ion temperature changes with beam energy or operation point on Q , verifying the method of researching the relationship between correction velocity and beam energy in Sec. III.

According to eq. (6), the importance of $(1/Q)dQ/dv$ should be recognized to reveal the dependence of δv on beam energy. As shown in Fig. 8, it is found that $\delta v/T_i$ is linear with $(1/Q)dQ/dv$ and that the fitting slopes of carbon, deuterium, and hydrogen are 7.599×10^6 (m/s)²/eV, 3.584×10^7 (m/s)²/eV, and 5.999×10^7 (m/s)²/eV, respectively. The calculated slopes of carbon, deuterium, and hydrogen with the ratio of Boltzmann constant to the mass of fully ionized ions k/m are 7.994×10^6 (m/s)²/eV, 4.769×10^7 (m/s)²/eV, and 9.593×10^7 (m/s)²/eV, respectively. The smaller the mass is, the larger the difference between fitting results and calculation is. The broadening of the spectra depends on the ratio of ion temperature and mass. Therefore, to some extent, the decreasing mass represents the increasing ion temperature and the influence of ion temperature on actual Q and $(1/Q)dQ/dv$ becomes different from eq. (6). Another possible explanation may be that the contribution of the curvature of Q as shown in eq. (5) plays a role though part of it is compensated by the square of the gradient of Q . Except for the linearity, there is the common feature that $\delta v/T_i$ becomes zero when $(1/Q)dQ/dv = 0$, which means that there would be no line shift due to the cross section if the cross section is independent of energy.

5. Summary and discussion

Based on the linear relationship between $\delta v/T_i$ and $(1/Q)dQ/dv$, the experimental normalized gradient of effective emission coefficient would have the same tendency as V_{cor}/T_i shown in Fig. 5. For the carbon system, compared with calculated $(1/Q)dQ/dv$ shown in Fig. 6 (a), the experimental $(1/Q)dQ/dv$ reaches the maximum at beam energy of 30 keV/amu and starts to decrease when beam energy decreases from 30 keV/amu to 20 keV/amu, while the calculated $(1/Q)dQ/dv$ continues increasing. However, for the hydrogen system, the experimental $(1/Q)dQ/dv$ of hydrogen (or deuterium) shows the same tendency as the calculation shown in Fig. 6 (b). The most likely reason why this occurs in the carbon system could be the underestimation of the calculation of Q in low beam energy region. Only the ground state donor is considered in the calculation. However, the cross section of $n=2$ excited state peaks at low beam energy and is much larger than



that of the ground state, resulting in a noticeable augment of effective emission coefficient even with a fraction of 0.1%.

For the $n=2$ excited state donor, the code “en2_kvi” with medium quality in the qcx#h0 library is used for carbon and “e2s” with low quality for hydrogen. Although the excited state donor of hydrogen includes both H(2S) and H(2P), the population of H(2P) is much smaller than that of H(2S). Therefore, Q of H(2S) is regarded as effective emission coefficient of $n=2$ excited state hydrogen. For Q between carbon and hydrogen as shown in Fig. 9 (a), there are no obvious variations between Q with and without $n=2$ excited state when beam energy is larger than 40 keV/amu. But the difference between them

becomes larger and larger when beam energy decreases from 40 keV/amu to 10 keV/amu, which leads to the decrease of Q gradient shown in Fig. 10 (a). However, for Q between hydrogen and hydrogen shown in Fig. 9 (b), the peaks of Q of ground state and n=2 excited state are overlapped by each other, leading to the same tendency of $(1/Q)dQ/dv$ shown in Fig. 10 (b). But it also can be found in both cases that Q increases with the increasing fraction of n=2 excited state. Considering the wide discharge conditions and the dependence of other parameters on Q, parameter scans are required to obtain the credible Q. According to the plasma condition, five sets of parameters are used as follows: (1) $T_e = T_i = 2$ keV, $n_e = 5 \times 10^{19} \text{ m}^{-3}$, (2) $T_e = T_i = 2$ keV, $n_e = 1 \times 10^{19} \text{ m}^{-3}$, (3) $T_e = T_i = 2$ keV, $n_e = 0.5 \times 10^{19} \text{ m}^{-3}$, (4) $T_e = T_i = 0.5$ keV, $n_e = 1 \times 10^{19} \text{ m}^{-3}$, and (5) $T_e = T_i = 10$ keV, $n_e = 1 \times 10^{19} \text{ m}^{-3}$, where T_e and n_e are electron temperature and electron density, respectively.

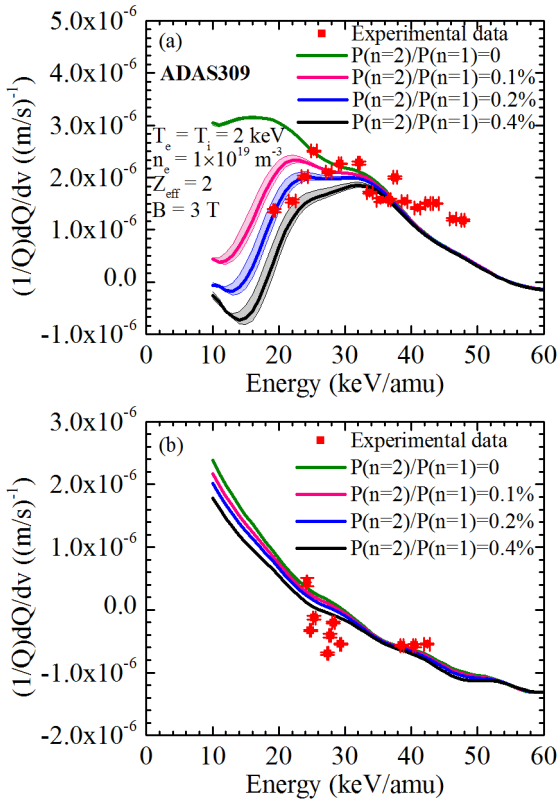


Fig. 10. Comparison between the normalized gradient of experiment and that of different fractions of the n=2 excited state with ADAS309 (a) carbon and (b) hydrogen

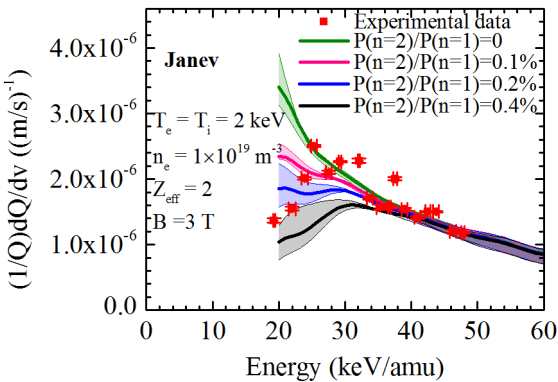


Fig. 11. Comparison between the normalized gradient of experiment and that of different fractions of n=2 excited state with Janev93 for carbon

Fig. 10 shows $(1/Q)dQ/dv$ with different fractions of n=2 excited state, together with the experimental $(1/Q)dQ/dv$ based on V_{cor}/T_i , where the shadow represents the region between the minimum and the maximum of $(1/Q)dQ/dv$. Only the maximum and the minimum of $(1/Q)dQ/dv$ are shown for each set of parameters. For the carbon system as shown in Fig. 10 (a), it is found that experimental $(1/Q)dQ/dv$ shows good agreement with that including n=2 excited state but that there is an underestimation of calculated $(1/Q)dQ/dv$ with ADAS when beam energy is larger than 38 keV/amu. As for the hydrogen system, it is seen in Fig. 10 (b) that the experimental $(1/Q)dQ/dv$ with increasing beam energy but that there is an overestimation of the calculation when beam energy is in the range of from 25 keV/amu to 30 keV/amu. This discrepancy may result from the accuracy of the atomic data for NBI provided by ADAS because the calculated cross section relies strongly on the collisional-radiative models of the beam [12, 13].

The first neutral beam models taking the excited state into account were developed by Boley *et al* [17] and Janev *et al* [18]. Therefore, in order to further evaluate the experimental $(1/Q)dQ/dv$, the cross section of Janev93 [19] is applied and the results with the same conditions as Fig. 10 (a) are shown in Fig. 11. It is found that the experimental $(1/Q)dQ/dv$ is consistent with the calculated $(1/Q)dQ/dv$ with Janev93 when beam energy is larger than 38 keV/amu. Combined with $(1/Q)dQ/dv$ from ADAS and that from Janev93, the non-monotonic tendency of experimental $(1/Q)dQ/dv$ of carbon verifies the non-negligible contribution of the n=2 excited state to the cross section at low beam energy and the fraction of the n=2 excited state is in the range of from 0.0% to 0.4%. It should be mentioned that the best fit curve to the experimental $(1/Q)dQ/dv$ is 0.2% of the n=2 excited state, which is similar to the fraction of 0.26% by Solomon *et al* [11]. For the hydrogen system, though the tendency of experimental and calculated $(1/Q)dQ/dv$ are the same, more investigations are required to obtain the reliable $(1/Q)dQ/dv$ from experiments due to the small dependency of $(1/Q)dQ/dv$ on the fraction of the n=2 excited state.

Based on the relationship between correction velocity and beam energy shown in Fig. 5, the correction to the flow velocity measurements has been applied on LHD. In comparison with calculated $(1/Q)dQ/dv$, considering the influence of the fraction of the excited state donor, it would be more appropriate to use the measured V_{cor} to correct the flow velocity measurements. It should be mentioned that the effect of the gyro motion of excited ions becomes significant at high magnetic field especially for the correction to the poloidal flow. In magnetized plasma, toroidal flow velocity is usually much larger than poloidal flow velocity. In the toroidal flow velocity measurements, the correction of flow velocity due to $V_{\text{perp}}^{\text{cor}}$ is not necessary because both the line of sight of the toroidal view and the neutral beam line are on the midplane. In contrast, the correction of flow velocity due to $V_{\text{perp}}^{\text{cor}}$ has been taken into account in the poloidal flow velocity measurements because the poloidal flow velocity becomes small and comparable or even smaller than

$V_{\text{perp}}^{\text{app}}$ in the core region where the ion temperature is high.

In conclusion, correction velocity due to the cross section effect is acquired by using the symmetric layout of poloidal CXS on LHD. A linear relationship between V_{cor} and T_i is observed. Large amounts of discharges with a wide plasma condition, including hydrogen and deuterium donors, are investigated and the relationships between V_{cor}/T_i of the carbon system and the hydrogen system and beam energy are discovered. The dependence of correction velocity on beam energy is discussed with the model of eq. (1) and it is found that what determines correction velocity is not Q itself but $(1/Q)dQ/dv$. The different behaviors of V_{cor} with carbon and hydrogen receivers are also discussed. On the basis of the linear relationship between $\delta v/T_i$ and $(1/Q)dQ/dv$ calculated with ADAS, experimental $(1/Q)dQ/dv$ is obtained according to the V_{cor}/T_i . The experimental $(1/Q)dQ/dv$ of the carbon system shows non-monotonic tendency with beam energy. But experimental $(1/Q)dQ/dv$ of the hydrogen system shows monotonic tendency. Combining $(1/Q)dQ/dv$ from ADAS and that from Janev93, the contribution of the $n=2$ excited state donor is verified.

Acknowledgments

The authors would like to thank the staff of LHD for their help with the experiments. This work is partly supported by JSPS KAKENHI Grant Numbers JP15H02336 and JP17H01368. This work is also partly supported by the National Institute for Fusion Science grant administrative budget NIFS10ULHH021 and by the State Scholarship Fund of CHINA SCHOLARSHIP COUNCIL.

References

[1] T.S. Hahm, Phys. Plasmas 1 (1994) 2940.
[2] K.H. Burrell, Phys. Plasmas 4 (1997) 1499.
[3] K. Ida, S. Kado, Y. Liang, Rev. Sci. Instrum. 71 (2000) 2360.

[4] M. Yoshinuma, K. Ida, M. Yokoyama, M. Osakabe, K. Nagaoka, Fusion Sci. Technol. 58 (2010) 375.
[5] Y.Y. Li, J. Fu, B. Lyu, X.W. Du, C.Y. Li, Y. Zhang, X.H. Yin, Y. Yu, Q.P. Wang, M. von Hellermann, Y.J. Shi, M.Y. Ye, B.N. Wan, Rev. Sci. Instrum. 85 (2014) 11E428.
[6] R.B. Howell, R.J. Fonck, R.J. Knize, K.P. Jaehnig, Rev. Sci. Instrum. 59 (1988) 1521.
[7] M.G. von Hellermann, W. Mandl, H.P. Summers, H. Weisen, A. Boileau, P.D. Morgan, H. Morsi, R. Koenig, M.F. Stamp, R. Wolf, Rev. Sci. Instrum. 61 (1990) 3479.
[8] R.E. Bell, E.J. Synakowski, AIP Conference Proceedings 547 (2000) 39.
[9] W.M. Solomon, K.H. Burrell, P. Gohil, R.J. Groebner, L.R. Baylor, Rev. Sci. Instrum. 75 (2004) 3481.
[10] R. Hoekstra, H. Anderson, F.W. Blied, M. von Hellermann, C.F. Maggi, R.E. Olson, P.H. Summers, Plasma Phys. Control. Fusion 40 (1998) 1541.
[11] W.M. Solomon, K.H. Burrell, R. Feder, A. Nagy, P. Gohil, R.J. Groebner, Rev. Sci. Instrum. 79 (2008) 10F531.
[12] E. Delabie, M. Brix, C. Giroud, R.J.E. Jaspers, O. Marchuk, M.G. O'Mullane, Yu. Ralchenko, E. Surrey, M.G. von Hellermann, K.D. Zastrow, Plasma Phys. Control. Fusion 52 (2010) 125008.
[13] I.H. Hutchinson, Plasma Phys. Control. Fusion 44 (2002) 71.
[14] J.M. Muñoz Burgos, K.H. Burrell, W.M. Solomon, B.A. Grierson, S.D. Loch, C.P. Balance, C. Chrystal, Nucl. Fusion 53 (2013) 093012.
[15] M. von Hellermann, P. Breger, J. Frieling, R. Konig, W. Mandl, A. Maas, H.P. Summers, Plasma Phys. Control. Fusion 37 (1995) 71.
[16] H.P. Summers, The ADAS User Manual version 2.6 www.adas.ac.uk (2004)
[17] C.D. Boley, R.K. Janev, D.E. Post, Phys. Rev. Lett. 52 (1984) 534.
[18] R.K. Janev, C.D. Boley, D.E. Post, Nucl. Fusion 29 (1989) 2125.
[19] R.K. Janev, J.J. Smith, Atomic Plasma Mater. Int. Data Fusion, Nucl. Fusion (suppl) (1993).